

# Prediction of odd-mode instabilities under output mismatch effects

Franco Ramírez, Almudena Suárez, Sergio Sancho

Communications Engineering Department, University of Cantabria  
Av. Los Castros s/n, 39005, Santander, Spain

**Abstract**—A methodology is presented to predict odd-mode instability in power amplifiers under output mismatch effects, as in the case of amplifiers connected to an antenna. This kind of instability is often observed in power-combining configurations, due to their symmetry properties. Unlike the single-ended situation, there is a cancellation of odd multiples of the oscillation frequency at the circuit output, so there is no impact of the load impedance values at the sideband frequencies. The odd-mode instability depends on the terminations at the fundamental frequency and its harmonic terms, and can only be detected within the circuit unstable loop, instead of the output plane. Here a methodology for the prediction and suppression of odd-mode instabilities is presented. Low-pass filtering effects and the use of a shorted stub allow the stability analysis to be limited to the fundamental-frequency termination. Then, the stability boundaries are efficiently determined through bifurcation detection inside the unstable loop, using the magnitude and phase of the reflection coefficient as the analysis parameters. Results have been validated through pole-zero identification and experimental measurements.

**Keywords**— *Stability, bifurcation, mismatch effect, power amplifier*

## I. INTRODUCTION

The instability of power amplifiers (PAs) under termination conditions other than  $50 \Omega$ , usually due to antenna mismatch [1-2], can lead to serious malfunctioning, involving the observation of incommensurable oscillations and frequency divisions [2]. To guarantee a reliable operation in a variety of conditions, some applications impose stable operation even under highly reflective loads [3]. In order to achieve this requirement, the works [4-5] provide criteria for unconditional instability under output mismatch effects, which are applicable to single-ended circuits. This stability analysis must be carried out under unknown values of the load impedance. Due to its frequency dependence, this impedance will be different at the fundamental frequency and its various harmonic components,  $mf_{in}$ , and sideband frequencies,  $mf_{in} + f$ , where  $m$  is an integer and  $f$  is a perturbation frequency, to be swept in the stability analysis [5]. Under fulfilment of an equivalent of the Rollet's proviso established in [5], the potential instability can be detected at the circuit-output reference plane, and due to the low-pass filtering action of the output network, the consideration of mismatch effects can be limited to  $f_{in}$  and the lowest sideband frequencies  $f$ ,  $-f_{in} + f$  and  $f_{in} + f$ , with all

the rest of components terminated in  $50 \Omega$ . The analysis in [5] predicts the possible observation of negative resistance at any of the three lowest sidebands under passive terminations at the other two sidebands, for all the possible values of the fundamental-frequency termination  $\Gamma_o$ . However, this method cannot be applied to circuit exhibiting odd-mode instabilities, often observed in circuits with symmetries, such as power combining PAs. This is because there is no observability of these instabilities at the circuit-output reference plane, due to their mathematical cancellations with right-hand side (RHS) zeroes [6]. They can only be detected through a stability analysis performed at the internal circuit nodes, under variation of the output impedance terminations at  $mf_{in}$ . The odd-mode instability often involves a subharmonic oscillation due to the influence of the input signal on the critical circuit frequencies, which are shifted to the divided-by-two frequency [7]. Here an efficient methodology for the detection of this kind of instability will be presented, taking into account the influence of the input power. The method will be illustrated through its application to a power-combining amplifier at  $f_{in} = 1.5 \text{ GHz}$ , which has been manufactured and measured.

## II. ANALYSIS METHOD

Let a circuit exhibiting symmetries, such as the one in Fig. 1, be considered. Under an odd-mode oscillation at the frequency  $f_a$ , all the intermodulation products of the form  $mf_{in} + (2n+1)f_a$ , where  $m$  and  $n$  are integers, will exhibit  $180^\circ$  phase shift in equivalent nodes and branches of the two sub-amplifiers, and will inherently cancel out at the circuit output. Despite this, the antenna impedance can affect the circuit odd-mode stability since it will alter the termination impedance at  $mf_{in}$ , which will give rise to a change in the steady-state solution  $\bar{X}_o$  about which the circuit is linearized in the stability analysis, where  $\bar{X}_o$  represents the vector of harmonic components of the circuit state variables. This situation in which the stability properties depend on the termination at  $mf_{in}$  but are independent on the terminations at the sideband frequencies at  $mf_{in}+f$  can also be interpreted as a failure of the proviso established in [5] (an extension of Rollet's proviso to the sideband-impedance problem). This is because the odd-mode instability will be observed even if the sideband frequencies are terminated in open or short circuits at the PA output [5].

This work has been funded by the Spanish Government under contract TEC2014-60283-C3-1-R, the European Regional Development Fund (ERDF/FEDER) and the Parliament of Cantabria (12.JP02.64069).

The odd-mode stability analysis under output mismatch effects will depend on the termination impedances at  $mf_{in}$ . However, due to inherent filtering effects, only the lower harmonic components will have an impact on these properties. To limit this impact to the fundamental frequency only, a  $180^\circ$  shorted stub at  $2f_{in}$  will be introduced in parallel with the final 50 Ohm load (the load that will undergo changes under the mismatch effects), which will eliminate the influence of the impedance terminations at the even harmonic terms. On the other hand, in practical applications one can expect a limited influence of the termination at the third harmonic component  $3f_{in}$ , since the power level of this spectral line is usually much lower than that at  $f_{in}$ . Thus, the stability properties will mostly depend on the fundamental-frequency termination  $\Gamma_o$ . The analysis test-bench is shown in Fig. 1, where harmonics  $|m|>1$  are terminated in 50 Ohms due to their limited influence.

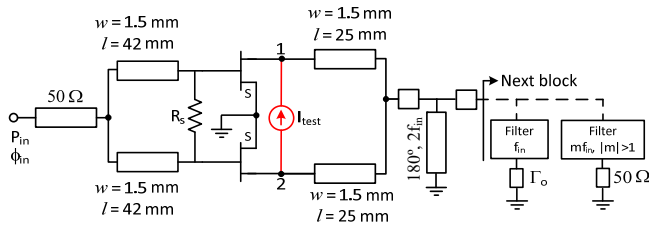


Fig. 1. Test-bench power amplifier based on a CLY5 transistor (RO4003C:  $\epsilon_r=3.38$ ,  $h=0.5$  mm). The original value of the stabilization resistor is  $R_s = 170 \Omega$ . The small-signal current source is introduced to evaluate the limit-oscillation conditions at an incommensurable frequency  $f$  or a subharmonic frequency  $f_{in}/2$  (which needs the consideration of the phase  $\phi_m$ ).

Under the above assumptions, pole-zero identification [6] would be applicable to detect the odd-mode instability under variations of  $\Gamma_o$ . This requires a connection of the small-signal source in parallel between the two circuit branches, since, in any other position (between one node and ground, for instance), a constant complex impedance ( $\Gamma_o$ ) at the sideband frequencies would not represent a physical behavior. Such an analysis would require a sweep in the perturbation frequency (going from 0 to  $f_{in}$  in periodic regimes), for each steady-state solution obtained through a double sweep in the amplitude and phase of  $\Gamma_o$ . Then, pole-zero identification should be applied to all the transfer functions resulting from this double sweep. The identification interval 0 to  $f_{in}$  should be, in general, divided into smaller intervals, so this analysis will be computationally demanding. Instead, the aim here will be to obtain directly the boundary between stable and unstable  $\Gamma_o$  values by tracing the bifurcation loci in the Smith Chart.

The Hopf-bifurcation locus [7-8] will provide the boundary of the load-impedance region for which the circuit exhibits an incommensurable oscillation. At the steady-state oscillation, the total admittance function  $Y_T$ , or current-to-voltage ratio, is equal to zero at all the circuit nodes. On the other hand, at the limit oscillation condition, the oscillation amplitude tends to zero. Taking these two conditions into account, the Hopf locus will be obtained by introducing a small-signal current source at the frequency  $f$  inside the potentially unstable loop (Fig. 1). Here it will be connected

between equivalent device nodes of the two subcircuits. For each  $P_{in}$ , the stability boundary is given by:

$$\bar{H}(\bar{X}_o, \rho_o, \phi_o) = 0, \quad Y_T(\bar{X}_o, \rho_o, \phi_o, f_{AG}) = 0 \quad (1)$$

where  $\bar{H} = 0$  is the whole set of harmonic-balance (HB) equations, acting as an inner tier, and  $\rho_o, \phi_o$  are the magnitude and phase of  $\Gamma_o$ . The steady-state solution  $\bar{X}_o$  depends on  $\Gamma_o$  and the limit oscillation condition,  $Y_T = 0$ , is evaluated with the conversion-matrix approach.

The analysis based on (1) should start with a global exploration of the Smith Chart, in order to provide a suitable initial value to the optimization/calculation procedure. This is done with a simple graphical technique that takes advantage of the bounded nature of  $\rho_o$  and  $\phi_o$ . The perturbation frequency  $f$  is swept between 0 and  $f_{in}$  and, for each  $f$ , a double sweep is performed in  $\rho_o, \phi_o$ , so as to cover the full Smith Chart. For each triplet  $f, \rho_o, \phi_o$ , the total admittance  $Y_T$  is calculated as the ratio between the current delivered by the small-signal source and the voltage across its terminals  $Y_T = I_{test}/(V_1 - V_2)$ . To fulfill  $Y_T = 0$ , there must be changes of sign in both the real and imaginary parts of  $Y_T$  under variations of  $\rho_o, \phi_o$ , which is easily evaluated by simple inspection. (An example is presented in Fig. 2). Initial values for the optimization should be close to  $Y_T = 0$ , and this situation may be found in one or several regions of the Smith Chart. This initial value (or values) should be introduced in system (1), which will provide an initial Hopf-locus point  $\rho_o^i, \phi_o^i, f^i$ . Then the whole locus will be efficiently traced through continuation, by sweeping  $\phi_o$  around  $\phi_o^i$  and solving (1) to obtain:  $\rho_o(\phi_o), f(\phi_o)$ . There will be one Hopf locus for each  $P_{in}$ .

One common case of odd-mode instability is the frequency division by 2, associated with flip bifurcations [7-8]. This phenomenon occurs when the input signal shifts the circuit natural frequency to one half the input frequency:  $f_a \rightarrow f_{in}/2$ , which is often associated with a parametric instability. This evolution involves the merging of a pair of complex-conjugate poles at  $f_a$  into two pairs of complex-conjugate poles at  $f_{in}/2$ , in order to preserve the system dimension [7]. At the division threshold, the subharmonic-oscillation amplitude will tend to zero, so the flip bifurcations can be detected by setting the frequency of the small-signal current source to  $f_{in}/2$ . Because this perturbation frequency ( $f_{in}/2$ ) and the input frequency are commensurable, the phase shift between the input source and the current source is a relevant analysis variable [9]. For the bifurcation detection, one can set the phase of the current source to zero and consider the input-source phase  $\phi_{in}$ . The mathematical conditions for the flip bifurcation are:

$$\bar{H}(\bar{X}_o, \rho_o, \phi_o, \phi_m) = 0, \quad Y_T(\bar{X}_o, \rho_o, \phi_o, \phi_m) = 0 \quad (2)$$

Unless a modified conversion-matrix analysis [9,10] is applied, the above analysis must be carried out with HB at the fundamental frequency  $f_{in}/2$ , due to the frequency commensurability. The initial value(s) is obtained through 3 nested sweeps, in the input-source phase  $\phi_{in}$ , varied between 0

and  $360^\circ$ , and in  $\rho_o, \phi_o$ , to cover the full Smith Chart. Once an initial point  $\rho_o^i, \phi_o^i, \phi_m^i$  has been obtained, the flip locus will be obtained through continuation, by sweeping the phase  $\phi_o$  around  $\phi_o^i$ , and solving (2) to obtain:  $\rho_o(\phi_o), \phi_m(\phi_o)$ . In amplifiers composed of several stages, the above methodology should be applied at each stage, and covering all the possible oscillation modes resulting from the circuit symmetry.

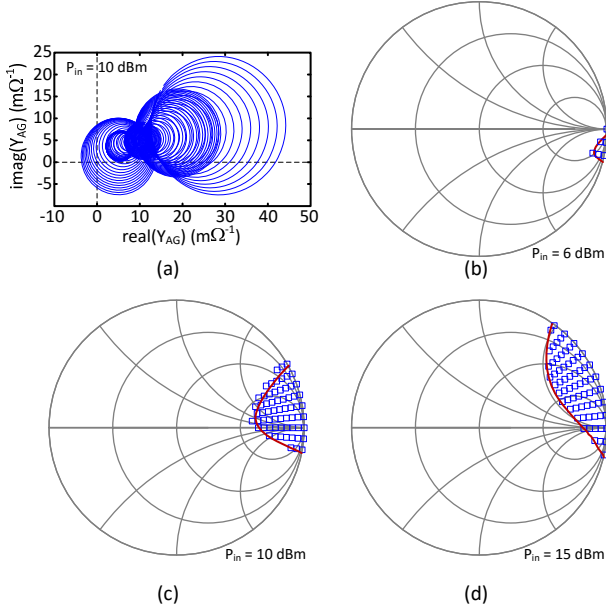


Fig. 2. Graphical method to obtain initial values. (a) Admittance diagram. (b) Region of points with  $\text{Re}(Y_T) < 0$  and  $|\text{Im}(Y_T)| \leq 10^{-3} \Omega^{-1}$  for  $P_{in} = 6$  dBm. (c) For  $P_{in} = 10$  dBm. (d) For  $P_{in} = 15$  dBm.

### III. APPLICATION TO A MISMATCHED AMPLIFIER

The above method has been applied to the circuit in Fig. 1. In the absence of mismatch effects, this amplifier is stable for all the  $P_{in}$  values, as verified with pole-zero identification [1,3,6]. On the other hand, the amplifier does not exhibit even-mode instabilities under mismatch effects, as verified with the method in [5]. The purpose here will be to predict the possible odd-mode instability under output mismatch effects. The admittance plots  $Y_T(\bar{X}_o, \rho_o, \phi_o, f)$  never cross the negative real semi-axis, so no incommensurable oscillation should be expected. The same analysis has been performed for the function  $Y_T(\bar{X}_o, \rho_o, \phi_o, \phi_m)$ , which provides several crossings of the negative real semi-axis [Fig. 2(a)], indicating the possible fulfillment of the flip-bifurcation condition (2). Actually, processing the data in Fig. 2(a) it has been possible to obtain the  $\Gamma_o$  values giving negative conductance ( $\text{Re}(Y_T) < 0$ ), with a magnitude of the imaginary part  $|\text{Im}(Y_T)|$  below  $10^{-3} \Omega^{-1}$  at different  $P_{in}$  values, represented with squares in Fig. 2(b-d).

Using an initial value from Fig. 2(a), the flip bifurcation loci in Fig. 3 have been obtained, where each locus corresponds to a different  $P_{in}$ . Because the amplifier is stable in matched conditions, the stable region corresponds to the

outside of the flip loci. For low  $P_{in}$ , the locus does not enter the Smith Chart, so there is unconditional stability. From  $P_{in} \cong 5$  dBm, the locus crosses the Smith Chart, so the amplifier is potentially unstable under mismatch effects. Due to the natural reduction of the negative resistance from certain signal amplitude, one should expect the loci to escape from the Smith Chart from a given  $P_{in}$  value. The loci corresponding to the various  $P_{in}$  values considered in Fig. 2 have also been represented in that figure, in a red solid line. The unstable region contains a subset of the points with negative real part of  $Y_T$  and low magnitude of the imaginary part. Note that the negative real part and positive-slope resonance of  $Y_T$  do not constitute a general instability condition. However, the limit steady-state oscillation condition in (1) and (2) is rigorous and should be fulfilled at any circuit node at the stability boundary. Because this condition only depends on the load value  $\Gamma_o$  at  $f_m$ , all the possible implementation of this load should give rise to the same kind of behavior, either stable or unstable. This has been validated for two different  $\Gamma_o$  values, one at each side of the flip-bifurcation locus obtained for  $P_{in} = 15$  dBm (in a solid red line in Fig. 3), indicated as  $\Gamma_{t1}$  and  $\Gamma_{t2}$  in Fig. 3. They are relatively close to the stability boundary to evaluate the degree of accuracy. Fig. 4(a) presents the results of an independent stability analysis based on pole-zero identification when  $\Gamma_{t1}$  and  $\Gamma_{t2}$  are implemented with an RL series network. Fig. 4(b) presents the results of the parallel-RL implementation. Poles of the  $\Gamma_{t1}$  ( $\Gamma_{t2}$ ) load are represented with blue (red) crosses. With the two different implementations, the load  $\Gamma_{t1}$  is stable and the load  $\Gamma_{t2}$  is unstable, in agreement with results from (2).

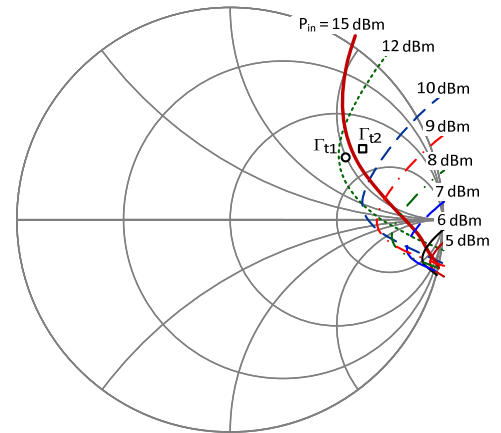


Fig. 3. Evolution of the flip locus obtained with (2) versus  $P_{in}$ . The loci only cross the Smith Chart in a certain  $P_{in}$  interval.

To determine the  $P_{in}$  interval with potential instability in an efficient manner, one can take into account the particular shape of the loci in Fig. 3. All the loci cross the boundary of the Smith Chart, so one can expect the locus to be tangent to this chart at the limits of the unstable  $P_{in}$  interval. This should be obtained for a magnitude of the reflection coefficient  $\rho_o = 1$ . The locus of  $P_{in}$  and  $\phi_o$  values fulfilling the flip-bifurcation condition under  $\rho_o = 1$  is expressed as:

$$\begin{aligned} \bar{H}(\bar{X}_o, \rho_o = 1, \phi_o, \phi_m, P_{in}) &= 0 \\ Y_T(\bar{X}_o, \rho_o = 1, \phi_o, \phi_m, P_{in}) &= 0 \end{aligned} \quad (3)$$

For  $P_{in}$  values such that the flip locus in (2) crosses the unit Smith Chart, there will be at least two  $\phi_b$  fulfilling (3) (Fig. 3). This is shown in Fig. 5, where the phase  $\phi_b$  at the intersection points with the Smith Chart [calculated with (3)] has been represented versus  $P_{in}$ . At the boundaries of the unstable  $P_{in}$  interval there will only be one  $\phi_b$ , since the locus is tangent to the Smith Chart. To stabilize the circuit under mismatch effects, the resistor  $R_s$  connected between the two amplifier branches will be reduced from its original value (170  $\Omega$ ). As expected (Fig. 5) the locus (3) decreases in size with  $R_s$  and eventually vanishes, due to the damping effect of this parallel resistor. For  $R_s < 120 \Omega$ , the amplifier should be stable for all the  $P_{in}$  values.

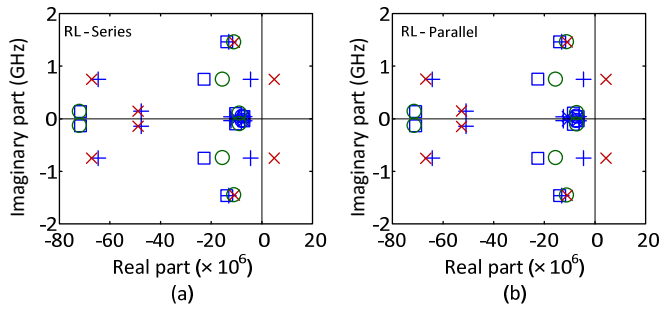


Fig. 4 Validation of the flip locus corresponding to  $P_{in} = 15$  dBm with two different implementations of  $\Gamma_{i1}$  and  $\Gamma_{i2}$  in Fig. 3. (a) RL-series implementation. Poles of the  $\Gamma_{i1}$  ( $\Gamma_{i2}$ ) load are represented with blue (red) crosses. (b) RL-parallel implementation. Poles of the  $\Gamma_{i1}$  ( $\Gamma_{i2}$ ) load are represented with blue (red) crosses.

The PA has been measured for two  $R_s$  values (150  $\Omega$  and 100  $\Omega$ ) and different positions of a triple-stub tuner, used to enable the load variation [Fig. 6(a)]. With  $R_s = 150 \Omega$ , the circuit is stable for the measured loads A and B and exhibits a frequency division by two for the loads C and D. See the spectra corresponding to B and C in Fig. 6(b) and 6(c). The low amplitude of the subharmonic spectral line is due to the near cancellation of this frequency component at the circuit output, due its odd-mode nature. The region of the unstable loads is in very good correspondence with the analysis in Fig. 3. With  $R_s = 100 \Omega$  the circuit is stable for all the load values [E,F,G,H are shown in Fig 6(a)] and all the  $P_{in}$  values, in agreement with Fig. 5.

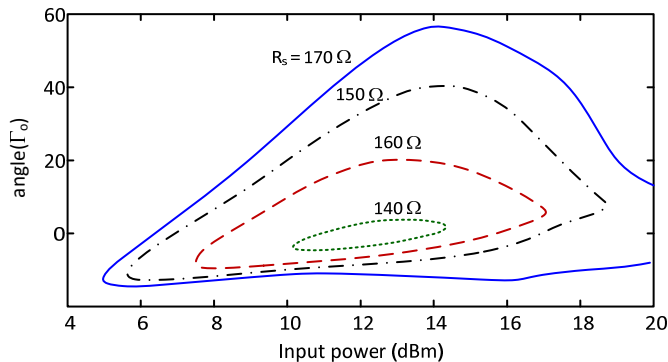


Fig. 5. Calculation of the unstable  $P_{in}$  interval using the locus in (3). The limit of this interval correspond to the edge points of the locus. The calculation has been repeated for different values of the stabilization resistor  $R_s$ .

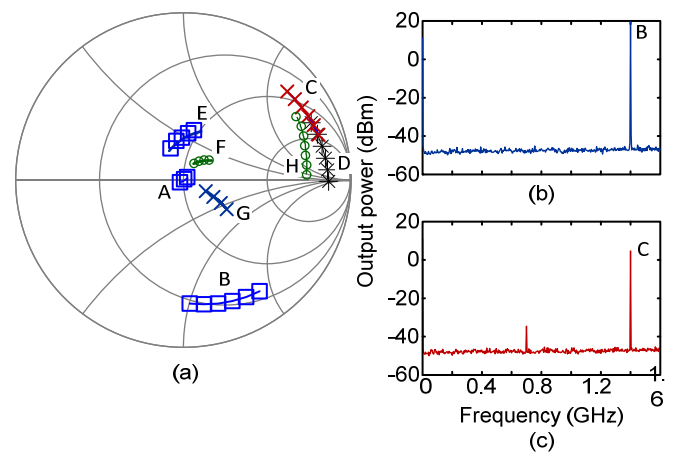


Fig. 6 Measurements for different positions of a triple-stub tuner. (a) The loads A,B,C,D correspond to tests under  $R_s = 150 \Omega$ . The loads E,F,G,H correspond to tests under  $R_s = 100 \Omega$ . (b) Spectrum for  $R_s = 150 \Omega$  and load B. (c) Spectrum for  $R_s = 150 \Omega$  and load C.

#### IV. CONCLUSION

A method has been presented to predict odd-mode instabilities in power amplifiers under output mismatch effects. It is based on tracing of the Hopf- and flip-bifurcation loci on the Smith Chart of the fundamental-frequency termination. The loci are calculated from a limit oscillation condition, evaluated at the unstable odd-mode loop. Initial values are efficiently obtained through a graphical method. Very good results have been obtained in the validation with pole-zero identification and with measurements.

#### REFERENCES

- [1] S. Dellier, R. Gourseyrol, J. Collantes, A. Anakabe, G. Soubercaze-Pun, K. Narendra, "Stability analysis of microwave circuits," *(WAMICON), 2012 IEEE 13th Annual*, pp.1-5, 15-17 Apr., 2012.
- [2] J. F. Imbornone, M. Murphy, R. S. Donahue and E. Heaney, "New insight into subharmonic oscillation mode of GaAs power amplifiers Under Severe Output Mismatch Condition," *IEEE Journal of Solid State Circuits*, vol. 32, pp. 1319-1325, Sept., 1997.
- [3] A. Anakabe, et al. "Automatic pole-zero identification for multivariable large-signal stability analysis of RF and microwave circuits," *European Microwave Conference (EuMC)*, Paris, pp. 477-480, 2010.
- [4] A. Suárez, F. Ramírez, S. Sancho, "Stability Analysis of Power Amplifiers Under Output Mismatch Effects," *IEEE Trans. Microw. Theory Techn.*, vol. 62, no. 10, pp. 2273-2289, Oct., 2014.
- [5] A. Suárez, F. Ramírez, S. Sancho, "Generalized stability criteria for power amplifiers under mismatch effects," *IEEE Trans. Microw. Theory Techn.*, vol. 63, no. 12, pp. 4415-4428, Dec, 2015.
- [6] N. Ayllon, J.M. Collantes, A. Anakabe, I. Lizarraga, G. Soubercaze-Pun, S. Forestier, "Systematic Approach to the Stabilization of Multitransistor Circuits", *IEEE Trans. Microwave Theory & Tech.*, 2011; 59, no. 8, 2073 - 2082.
- [7] A. Suárez, Analysis and design of autonomous microwave circuits, IEEE-Wiley, Jan. 2009.
- [8] V. Rizzoli and A. Neri, "State of the art and present trends in nonlinear microwave CAD techniques," *IEEE Trans. Microw. Theory Techn.*, vol. 36, pp. 343-356, Feb., 1988.
- [9] F. Di Paolo, G. Leuzzi, "Bifurcation synthesis by means of Harmonic Balance and Conversion Matrix," *Proceedings of the European Gallium Arsenide Applications Symposium*, Munich, Oct., 2003, pp.521-524.
- [10] L. Pantoli, A. Suárez, G. Leuzzi, F. Di Paolo, "Complete and systematic simulation tools for frequency divider design," *IEEE Trans. Microw. Theory Techn.*, vol. 56, no. 11, pp. 2442-2452, Nov., 2008.